

Thomas-Fermi and Thomas-Fermi-Dirac calculations for atoms in a very strong magnetic field

B. Banerjee

Tata Institute of Fundamental Research, Bombay, India

D. H. Constantinescu

Institut für Theoretische Physik der Universität, Heidelberg, Germany

P. Reháč*

Institut für Experimentelle Kernphysik der Universität and Kernforschungszentrum, Karlsruhe, Germany

(Received 28 February 1974)

A statistical model for atoms in a very strong magnetic field (10^{12} – 10^{14} G) may be built, starting from the assumption that the Coulomb motion of the atomic electrons is adiabatically slow with respect to their magnetic motion. Within this framework, the binding energies and radii, as well as the ionization energies of singly and doubly ionized atoms, are computed for atomic numbers $5 \leq Z \leq 100$ in the Thomas-Fermi case, and for $5 \leq Z \leq 70$ in the Thomas-Fermi-Dirac case. Possible astrophysical implications may concern the emission of electrons and ions from the surface of pulsars, the abundances of the elements in the cosmic radiation, and the properties of the condensed matter forming the outer crust of magnetic neutron stars.

I. INTRODUCTION

The standard models for pulsars (rotating magnetic neutron stars) and the commonly accepted scenarios describing their formation (contraction during a supernova event, with conservation of the magnetic flux) point to magnetic fields of the order of 10^{12} – 10^{13} G at their surface. If this is indeed the case, the properties of matter at the surface of a pulsar¹ are very different from those of ordinary matter, due to the fact that the energies associated with the magnetic motion of electrons become much larger than their Coulomb energies.

Of the oscillatorlike energy levels corresponding to the motion of an electron perpendicularly to such an enormous magnetic field, practically only the lowest-lying one plays a significant role in the description of the properties of matter¹: As the spacing of the magnetic levels is of the order of the electron's rest mass and temperatures² are lower than 10^5 °K, the excitation of higher levels is negligibly small. The states corresponding to this ground level³ are conveniently chosen to be the eigenstates of the angular momentum along the magnetic field, with nonpositive eigenvalues $-\mu$ ($\mu = 0, 1, 2, \dots$); they have spin antiparallel to the field, and zero excitation of the radial motion. The density of probability in such a μ state is sharply peaked at a value of the radial coordinate equal to the cyclotron radius⁴

$$\rho_\mu = [(2\mu + 1)/eB]^{1/2}. \quad (1)$$

A relatively simple model for an N -electron ion

of atomic number Z can be built if one separates the transverse and longitudinal (with respect to the direction of the magnetic field) motions of the electrons. In this scheme, the transverse motion is determined by the magnetic field alone, the electrons having at their disposal the μ states described above. The Coulomb field of the nucleus determines only the longitudinal motion; the corresponding available states⁵ consist of a very deep ground level and of excited parity doublets situated very close to the normal Coulomb levels. This separation is a good assumption only if the cyclotron radius of the outermost electron is much smaller than its Bohr radius in an atom of atomic number Z :

$$\rho_{\mu_{\max}} \ll a_0/Z. \quad (2)$$

It then represents the well-known adiabatic approximation.

The distribution of the electrons among the transverse and longitudinal states, in the ground state of such an atom, is determined by the requirement that the energy be minimum, and depends upon Z , N , and the magnetic field. The following two situations represent opposite limiting cases of this distribution^{6,7} (the intermediate region has not been explored quantitatively):

(i) *Superstrong magnetic field.* If the condition (2) is satisfied for $\mu_{\max} \geq N$, the electrons will fill the successive μ states, all of them being in the deep ground longitudinal state (and therefore having nodeless longitudinal wave functions, highly peaked near the nucleus). A Hartree calculation^{8–10} shows that in this case atoms have very elongated

cylindrical shapes, small dimensions, and enormous binding energies. Their ionization energies change slowly and monotonically with the atomic number.

(ii) *Medium-strong magnetic field.* If inequality (2) holds only for $0 \leq \mu_{\max} \ll N$, practically all the electrons are in excited longitudinal states. The corresponding wave functions have nodes, the density of charge along the magnetic field is no longer maximum near the nucleus, which makes possible a description in terms of a statistical model. Such a model has been discussed in Refs. 6 and 7: Atoms are found to have spherical shapes, and their dimensions and energies to depend more strongly on the magnetic field than in the superstrong case. In these calculations the exchange interaction has been neglected; therefore they cannot be used to evaluate the ionization energies, which are very sensitive to exchange effects.

The purpose of the present work is precisely to incorporate exchange into the statistical model, in order to obtain a reliable estimate not only of the atomic dimensions and binding energies in the medium-strong range, but also of the ionization energies. To prepare the ground for the main calculation, we examine first the statistical model without exchange (Sec. II), and obtain a more complete and accurate solution of the Thomas-Fermi differential equation, compared with Refs. 6 and 7. The principal part of the paper is represented by Sec. III; here we compute the exchange contribution to the energy, then solve the corresponding Thomas-Fermi-Dirac equation and discuss the results in detail. A few concluding remarks are made in Sec. IV.

Natural units ($\hbar = c = 1$) are used throughout. The mass and the charge of the electron are denoted by m and e , respectively. Lengths are measured in Bohr units $a_0 = 1/m\alpha$, and energies in Rydberg units $m\alpha^2/2$, where $\alpha = e^2$ is the fine-structure constant. We use as a natural unit of magnetic field $B_c = m^2/e \approx 4.4 \times 10^{13}$ G, and express the field strength in terms of the dimensionless parameter

$$L = B/B_c = eB/m^2. \quad (3)$$

Cylindrical coordinates $\vec{r} = (\vec{\rho}, z)$ with the z axis directed along the magnetic field are used in some intermediate calculations.

II. STATISTICAL MODEL WITHOUT EXCHANGE

A. Kinetic energy

In expressing the kinetic energy of the atom in terms of the volume density of electrons, we make explicit use of the adiabatic hypothesis.

First, to relate the electron density to the Fermi momentum, we count the number of states inside a small volume which is conveniently taken to have the shape of a thin cylindrical shell of radius ρ , thickness $\Delta\rho$, and height Δz . The transverse states correspond (in the adiabatic approximation) to cyclotron orbits having radii given by Eq. (1); hence, the number of transverse states inside $\Delta\rho$ is $\Delta N_{\perp} = \Delta\mu = eB\rho\Delta\rho$. The longitudinal motion is treated statistically: As the electron density along z is a smooth function, the motion may be described, inside the small interval Δz , by a superposition of plane waves

$$f_q(z) = (\Delta z)^{-1/2} \exp(iqz), \quad (4)$$

with $|q| \leq q_F(\vec{r})$, where $q_F(\vec{r})$ is the Fermi momentum. The number of longitudinal states inside Δz is then $\Delta N_{\parallel} = (q_F/\pi)\Delta z$. Therefore, our cell of volume $\Delta V = 2\pi\rho\Delta\rho\Delta z$ can accommodate, according to the Pauli principle, a number $\Delta N = \Delta N_{\parallel}\Delta N_{\perp} = (eBq_F/2\pi^2)\Delta V$ of electrons, i.e., the density of electrons is

$$n(\vec{r}) = \frac{eB}{2\pi^2} q_F(\vec{r}). \quad (5)$$

Second, in the expression of the kinetic energy we keep only the contribution of the longitudinal motion. Indeed, the energy of the atom is, by definition, the energy of all the electrons bound together by the Coulomb field of the nucleus, minus their energy when they are free but still in the magnetic field, and this latter quantity cancels (in the adiabatic approximation) the kinetic energy of their transverse motion inside the atom. Thus, the kinetic energy of the electrons in our cell is simply

$$\begin{aligned} \Delta K &= \Delta N_{\perp} \frac{\Delta z}{2\pi} \int_{|q| \leq q_F} dq \frac{q^2}{2m} \\ &= \frac{eB}{(2\pi)^2} \frac{q_F^3}{3m} \Delta V. \end{aligned} \quad (6)$$

The density of kinetic energy is therefore, from Eq. (5),

$$k(\vec{r}) = \frac{2\pi^4}{3m(eB)^2} n^3(\vec{r}). \quad (7)$$

B. Thomas-Fermi equation

Having obtained a relationship between the kinetic energy density and the electron density, one can write the energy of a (Z, N) atomic ion as⁷

TABLE I. Solution of the TF equation: initial slope and position of the zero.

| Z | N = Z - 1 | | N = Z - 2 | |
|-----|---------------|--------------|---------------|--------------|
| | $\Phi'(0)$ | x_0 | $\Phi'(0)$ | x_0 |
| 5 | -0.942 017 69 | 2.114 384 60 | -0.957 547 13 | 1.754 521 79 |
| 6 | -0.940 932 16 | 2.185 234 99 | -0.950 193 57 | 1.867 209 58 |
| 7 | -0.940 331 34 | 2.239 812 44 | -0.946 438 05 | 1.950 967 02 |
| 8 | -0.939 966 38 | 2.283 565 84 | -0.944 275 68 | 2.016 530 37 |
| 9 | -0.939 728 35 | 2.319 812 24 | -0.942 919 59 | 2.069 883 27 |
| 10 | -0.939 565 34 | 2.350 442 31 | -0.942 017 69 | 2.114 384 60 |
| 11 | -0.939 448 74 | 2.376 873 31 | -0.941 388 06 | 2.152 341 68 |
| 12 | -0.939 362 74 | 2.399 964 54 | -0.940 932 16 | 2.185 234 99 |
| 13 | -0.939 297 65 | 2.420 353 47 | -0.940 591 94 | 2.214 125 48 |
| 14 | -0.939 247 06 | 2.438 613 43 | -0.940 331 34 | 2.239 812 44 |
| 15 | -0.939 207 13 | 2.455 037 36 | -0.940 127 96 | 2.262 813 31 |
| 16 | -0.939 174 94 | 2.470 000 00 | -0.939 966 38 | 2.283 565 84 |
| 17 | -0.939 148 78 | 2.483 619 38 | -0.939 835 53 | 2.302 488 04 |
| 18 | -0.939 127 20 | 2.496 124 85 | -0.939 728 35 | 2.319 812 24 |
| 19 | -0.939 109 11 | 2.507 713 68 | -0.939 639 62 | 2.335 733 46 |
| 20 | -0.939 093 92 | 2.518 418 94 | -0.939 565 34 | 2.350 442 31 |
| 25 | -0.939 044 66 | 2.562 409 52 | -0.939 328 09 | 2.410 445 33 |
| 30 | -0.939 019 03 | 2.595 406 34 | -0.939 207 13 | 2.455 037 36 |
| 35 | -0.939 004 06 | 2.621 432 56 | -0.939 137 49 | 2.490 000 00 |
| 40 | -0.938 994 59 | 2.642 711 92 | -0.939 093 92 | 2.518 418 94 |
| 45 | -0.938 988 23 | 2.660 531 54 | -0.939 064 92 | 2.542 149 57 |
| 50 | -0.938 983 76 | 2.675 808 37 | -0.939 044 66 | 2.562 409 52 |
| 55 | -0.938 980 50 | 2.689 037 06 | -0.939 029 97 | 2.580 000 00 |
| 60 | -0.938 978 05 | 2.700 758 03 | -0.939 019 03 | 2.595 406 34 |
| 65 | -0.938 976 17 | 2.711 129 95 | -0.939 010 64 | 2.609 114 11 |
| 70 | -0.938 974 69 | 2.720 498 05 | -0.939 004 06 | 2.621 432 56 |
| 75 | -0.938 973 50 | 2.729 000 00 | -0.938 998 83 | 2.632 569 15 |
| 80 | -0.938 972 55 | 2.736 703 43 | -0.938 994 59 | 2.642 711 92 |
| 85 | -0.938 971 76 | 2.743 792 75 | -0.938 991 11 | 2.652 000 00 |
| 90 | -0.938 971 10 | 2.750 288 35 | -0.938 988 23 | 2.660 531 54 |
| 95 | -0.938 970 55 | 2.756 337 55 | -0.938 985 81 | 2.668 435 27 |
| 100 | -0.938 970 08 | 2.762 000 00 | -0.938 983 76 | 2.675 808 37 |

$$\begin{aligned}
E &= K + V + W \\
&= \frac{2\pi^4}{3m(eB)^2} \int n^3(\vec{r}) d\vec{r} \\
&\quad - Ze^2 \int \frac{n(\vec{r})}{r} d\vec{r} \\
&\quad + \frac{e^2}{2} \int \frac{n(\vec{r})n(\vec{r}')}{|\vec{r} - \vec{r}'|} d\vec{r} d\vec{r}', \tag{8}
\end{aligned}$$

the meaning of the various terms being evident. To find the ground state of the atom, this expression is minimized as a functional of $n(\vec{r})$, subject to the condition that the total electronic charge be the right one:

$$N = \int n(\vec{r}) d\vec{r}. \tag{9}$$

Introducing a Lagrange multiplier $-e\varphi_0$, we require therefore that

$$\delta(E - e\varphi_0 N) = 0, \tag{10}$$

which yields the Thomas-Fermi (TF) integro-differential equation^{6,7}

$$\frac{2\pi^4}{m(eB)^2} n^2(\vec{r}) + e[\varphi(\vec{r}) - \varphi_0] = 0; \tag{11}$$

here

$$\varphi(\vec{r}) = -\frac{Ze}{r} + e \int \frac{n(\vec{r}')}{|\vec{r} - \vec{r}'|} d\vec{r}'. \tag{12}$$

Following closely the procedure used in the conventional statistical model (zero magnetic field)¹¹ we replace Eq. (11) by a differential equation by remarking that $\varphi(\vec{r})$ is the Coulomb potential due to the nucleus and the distribution of electronic charge around it, and therefore obeys the Poisson equation

$$\Delta\varphi(\vec{r}) = -4\pi en(\vec{r}), \tag{13}$$

and the boundary condition

$$\lim_{r \rightarrow 0} r\varphi(\vec{r}) = -Ze. \quad (14)$$

Now Eqs. (11) and (13) are combined to eliminate one of the functions $n(\vec{r})$ and $\varphi(\vec{r})$. As the boundary conditions are easier formulated in terms of the potential, we choose the customary way of eliminating $n(\vec{r})$. A considerable simplification is brought in by the theorem⁷ stating that the density $n(\vec{r})$ which minimizes the energy is spherically symmetric; then we are left with only one variable, $r = |\vec{r}|$. It is convenient to introduce a dimensionless variable x given by

$$r = a_0 2^{-3/5} \pi^{2/5} \alpha^{4/5} Z^{1/5} L^{-2/5} x, \quad (15)$$

and a new function

$$\Phi(x) = -\frac{r}{Ze} [\varphi(r) - \varphi_0]. \quad (16)$$

Then, from Eqs. (11) and (13) we obtain the TF differential equation

$$\Phi'' = (x\Phi)^{1/2}; \quad (17)$$

the boundary condition (14) becomes simply

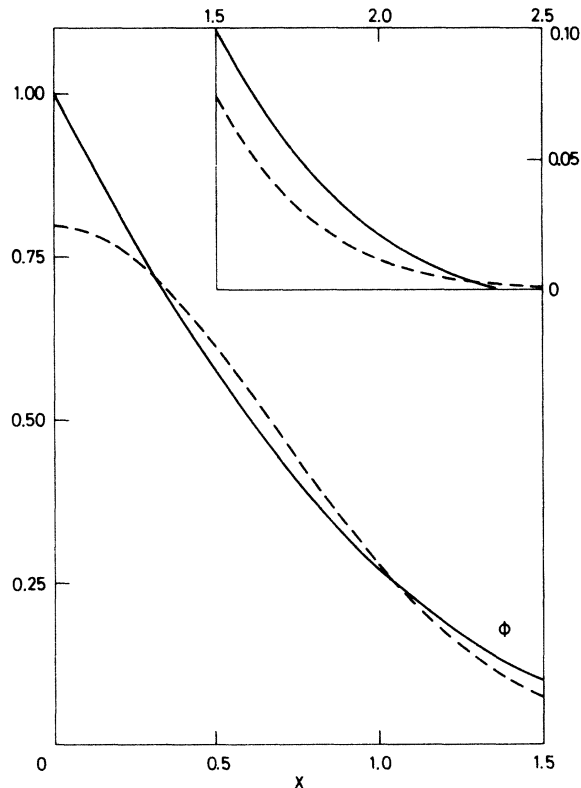


FIG. 1. Solution of the TF equation for $Z = 10$ and $N = 9$ (solid curve), and the corresponding MRS solution (dashed curve).

$$\Phi(0) = 1. \quad (18)$$

The family of solutions of Eqs. (17) and (18), corresponding to the various values of the initial slope $\Phi'(0)$, has qualitative properties similar to the analogous functions of the conventional TF model. All the solutions start from the origin with the value unity, and a positive curvature. Their behavior at large x depends upon $\Phi'(0)$; here one may distinguish three cases.

(i) If $\Phi'(0)$ is sufficiently negative, $\Phi(x)$ vanishes at a finite distance x_0 ; the corresponding r_0 is the atomic radius, where $n(r)$ vanishes. For $x > x_0$ the TF equation no longer holds, since this would imply a negative density of electrons.

(ii) For a less negative $\Phi'(0)$ there is one solution asymptotic to the x axis ($x_0 = \infty$).

(iii) For still higher initial slopes the solutions never vanish, but diverge as $x \rightarrow \infty$.

To select the unique solution corresponding to a given type of ion, we must add the requirement that the atom contains, inside the radius r_0 , defined by Eq. (15) and

$$\Phi(x_0) = 0, \quad (19)$$

the right charge. Using successively Eqs. (9), (13), and (16), one has

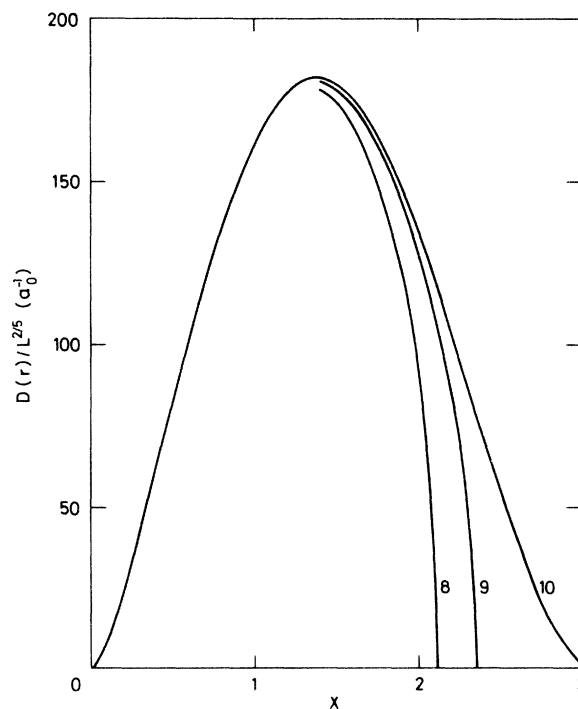


FIG. 2. Radial distributions of charge (divided by $L^{2/5}$), for $Z = 10$ and $N = 8, 9, 10$ (TF calculation).

$$\begin{aligned}
N &= 4\pi \int_0^{r_0} n(r)r^2 dr \\
&= -\frac{1}{e} \int_0^{r_0} \Delta\varphi(r)r^2 dr \\
&= Z \int_0^{x_0} \frac{d}{dx} [x\Phi'(x) - \Phi(x)] dx, \quad (20)
\end{aligned}$$

i.e.,

$$\Phi(x_0) - x_0\Phi'(x_0) = 1 - \frac{N}{Z}. \quad (21)$$

One notes that Eq. (17), the boundary conditions (18) and (21), and the definition of the atomic radius, Eq. (19), are all independent of the magnetic field, which appears only as a scaling factor for lengths, in Eq. (15): When L increases, all ions contract at the same rate. If $N=Z$ the equations are also independent of Z , so that there exists one universal solution for all neutral atoms, which is precisely the solution described above as case (ii); indeed, for neutral atoms Eqs. (19) and (21) imply $x_0 = \infty$. For positive ions ($N < Z$), the same equations are satisfied by a finite x_0 , and one is in case (i). Negative ions cannot be handled in this model, since the boundary conditions cannot be satisfied for $N > Z$. For free ions, case (iii) does not occur: Solutions of this type

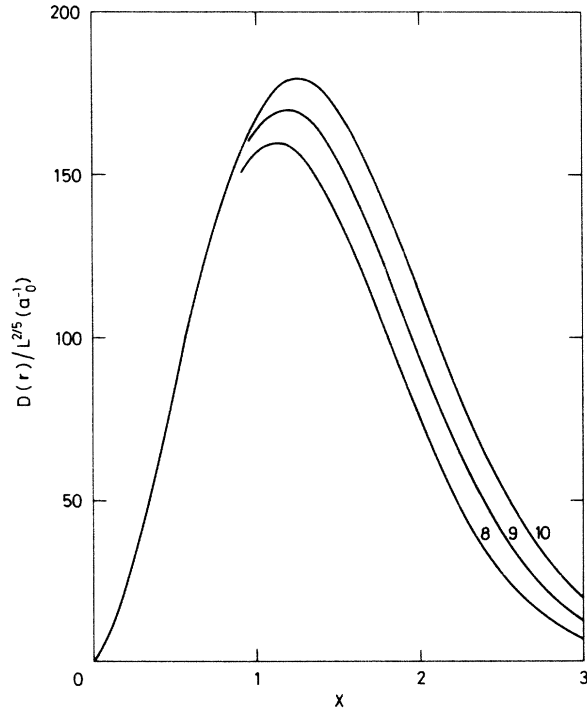


FIG. 3. Radial distributions of charge (divided by $L^{2/5}$), for $Z = 10$ and $N = 8, 9, 10$ (MRS calculation).

correspond to atoms under pressure (e.g., atoms squeezed together to form condensed matter), which we do not discuss here.

Once the solution of the TF equation is known, the atomic radius is given by Eq. (15). The electron density is obtained by combining Eqs. (11) and (16) to get

$$n(r) = a_0^{-3} 2^{-1/5} \pi^{-11/5} \alpha^{-12/5} Z^{2/5} L^{6/5} [\Phi(x)/x]^{1/2}. \quad (22)$$

Substituting this into Eq. (8), and after some manipulations (involving partial integrations and the use of the TF equation and the boundary conditions), the energy may be written in the form

$$E = -\frac{1}{2} m \alpha^{28/5} \pi^{-2/5} \alpha^{-4/5} Z^{9/5} L^{2/5} \epsilon, \quad (23)$$

where

$$\epsilon = -\frac{5}{9} \left[\Phi'(0) + \frac{1}{x_0} \left(1 - \frac{N}{Z} \right)^2 \right]. \quad (24)$$

Then, one can compute the binding energy of the last electron (ionization energy):

$$I(Z, N) = E(Z, N-1) - E(Z, N). \quad (25)$$

We mention here two additional relations between the various contributions to the energy: K , V , and W . One is the virial theorem⁷

$$6K + V + W = 0, \quad (26)$$

which may be checked directly. The other one tells that the entropy of the electron gas is zero (we have assumed zero temperature); it is ob-

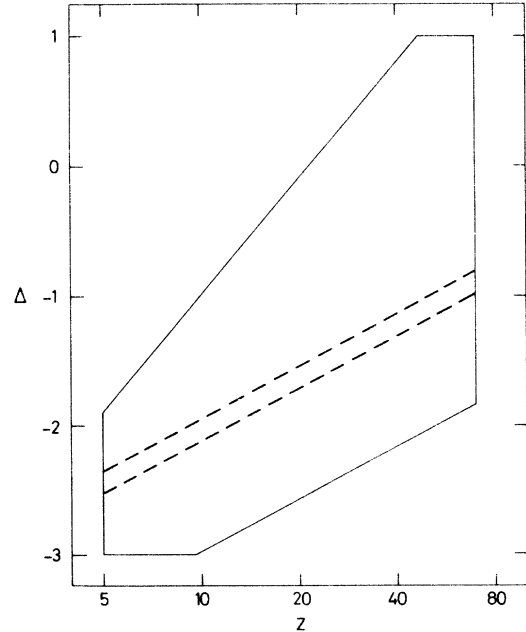


FIG. 4. Range covered by the TFD calculation; along the strip the virial theorem is obeyed exactly.

tained by multiplying Eq. (11) by $n(\vec{r})$ and then integrating:

$$3K + V + 2W = e\varphi_0 N. \tag{27}$$

The value of the multiplier φ_0 results from Eq. (11) for $r = r_0$:

$$\varphi_0 = \varphi(r_0) = -\frac{(Z - N)e}{r_0}. \tag{28}$$

These are simple consequences of the TF equation, but it is worth mentioning them, because their analogs for the statistical model with exchange offer the possibility of checking the accuracy of the approximation used there (see Sec. III).

The range of validity of the model has an upper limit given by the condition [see Eq. (1)]

$$\rho_Z \gg a_0/Z, \tag{29}$$

which ensures that practically all the electrons stay in excited states of the longitudinal motion. A lower limit comes from the requirement that the Coulomb energy of an electron at the periphery of the atom be small with respect to the spacing

of the magnetic levels:

$$|e\varphi(r_0)| \approx \frac{Ze^2}{r_0} \ll \frac{eB}{m}. \tag{30}$$

To evaluate this limit we set roughly $x_0 \approx 1$; then Eqs. (29) and (30) yield a range

$$5 \times 10^{-5} Z^{4/3} \ll L \ll 10^{-4} Z^3. \tag{31}$$

C. Numerical results

The TF equation was solved numerically in the range $5 \leq Z \leq 20$ (steps of 1), $20 \leq Z \leq 100$ (steps of 5), and $Z - 2 \leq N \leq Z$.

The universal solution corresponding to neutral atoms ($N = Z$) was found to have

$$\Phi'(0) = -0.938\ 965\ 94, \quad x_0 = \infty; \tag{32}$$

the value of the initial slope and the position of the zero for once- and twice-ionized atoms are given in Table I. This is all the information needed for calculating the atomic sizes and energies, as well as the ionization energies for the Z th and $(Z - 1)$ th electrons, using Eqs. (15) and (23)–(25).

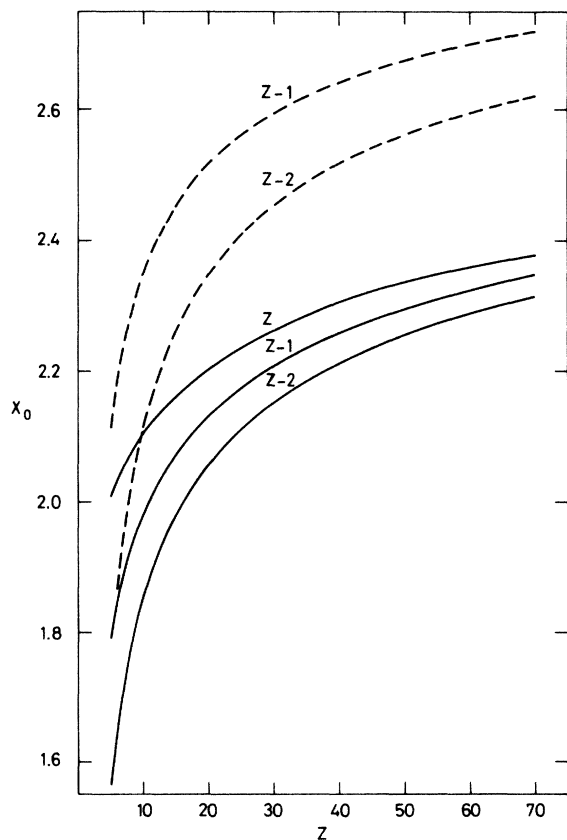


FIG. 5. Graphs of x_0 vs Z along the virial strip, for $N = Z - 2, Z - 1, Z$ (TFD calculation, solid curves); graphs of x_0 vs Z , for $N = Z - 2, Z - 1$ (TF calculation, dashed curves).

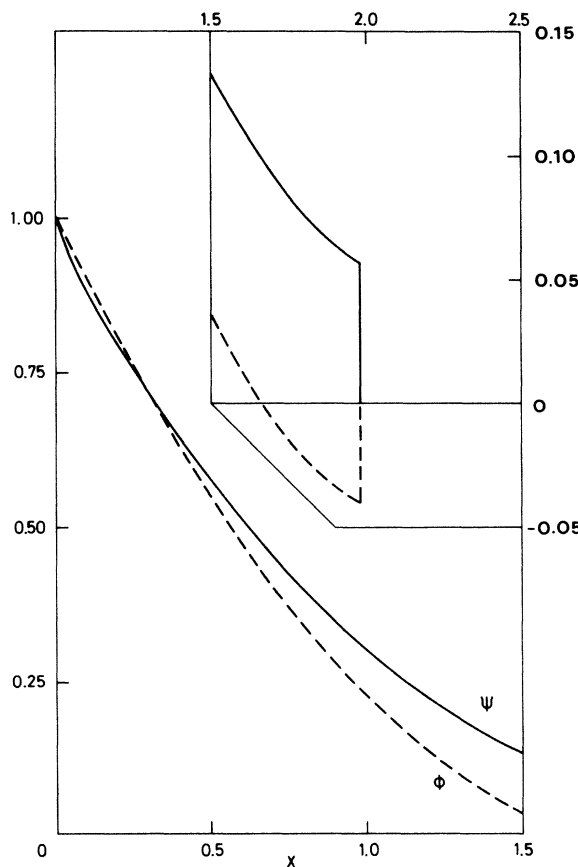


FIG. 6. Solution of the TFD equation for $Z = 10, N = 9$, and $\Delta = -2$.

An inspection of Table I reveals that near the origin the solutions for all Z 's and N 's are almost equal, and they begin to differ significantly only very close to x_0 .¹² To give a quantitative idea about the behavior of these solutions, Fig. 1 shows the function $\Phi(x)$ corresponding to $Z = 10$, $N = 9$.

More interesting than the solution $\Phi(x)$ itself is the distribution of the electronic charge inside the atom, viz. the quantity

$$D(r) = 4\pi r^2 n(r), \quad (33)$$

which gives the radial distribution of charge. In Fig. 2 the function $D(r)/L^{2/5}$ is plotted against x , for $Z = 10$ and $N = 8, 9, 10$. We see that the main contribution to the energy comes from the intermediate region around $x = 1.5$, where the function $\Phi(x)$ is already small; although $\Phi(x)$ is maximum at the origin, where the volume density of electrons becomes singular, the contribution of this interval is removed by the factor r^2 . Looking at Fig. 1 one realizes that an infinite x_0 for neutral atoms does not mean that in the TF model neutral atoms have infinite radius: Unlike in the conventional case, our distribution of charge does not have a long tail.¹³

It is instructive to compare these results with those yielded by the approximate solution of Mueller, Rau, and Spruch⁷ (MRS). Instead of solving the TF equation, these authors use a variational approach based on the following two *Ansätze*. First, as the distribution of charge is spherically-symmetric, the problem contains one length, which gives the size of this sphere of electronic charge. Calling R this unknown length, MRS satisfy Eq. (9) by setting

$$n(r) = \frac{N}{R^3} \rho(\xi), \quad \xi = \frac{r}{R}. \quad (34)$$

With this parametrization the energy, Eq. (8), becomes a function of R , and the requirement that it be minimum yields the solution

$$R = a_0 (4\pi^4 k)^{1/5} \left(v - \frac{N}{Z} w \right)^{-1/5} \alpha^{4/5} Z^{-1/5} N^{2/5} L^{-2/5},$$

$$E = -\frac{m\alpha^2}{2} \frac{5}{3} (4\pi^4 k)^{-1/5} \left(v - \frac{N}{Z} w \right)^{6/5} \times \alpha^{-4/5} Z^{6/5} N^{3/5} L^{2/5}; \quad (35)$$

the values of the constants k , v , and w depend on the choice of the function $\rho(\xi)$. Second, $\rho(\xi)$ is chosen in such a way as to satisfy approximately the boundary conditions for $n(r)$, i.e., have the right singularity at the origin, and a fast decrease at large distances. MRS assume

$$\rho(\xi) = C \xi^{-1/2} e^{-\xi^2}, \quad (36)$$

and obtain $4\pi^4 k = 7.12$, $v = 1.35$, $w = 0.33v$.

Obviously, a charge density given by Eqs. (34)–(36) satisfies neither the TF equation nor the correct boundary conditions. This is shown in Fig. 1, where the function $\Phi(x)$ corresponding to the MRS solution for $Z = 10$, $N = 9$ is compared with the exact $\Phi(x)$ given by the TF equation. However, we have seen that the relevant quantity is not $\Phi(x)$, but the radial distribution $D(r)$. Figure 3 shows the function $D(r)/L^{2/5}$, as given by MRS, for $Z = 10$ and $N = 8, 9, 10$; a comparison with Fig. 2 tells us that the MRS solution should yield accurate values for the energy, and indeed they differ from the exact ones by less than 1%. Atomic radii are too small by a factor of about 2, but this is a matter of definition: As in the MRS picture the charge density vanishes only at infinity, the “radius” R is defined by the half-width of the Gaussian-type distribution of Eq. (36). Ionization energies in the MRS model are higher than the TF ones by 10–30% (the error increases with Z).

Incidentally, we remark that the TF model, ignoring exchange, cannot yield reliable values of the ionization energies. Indeed, exchange ef-

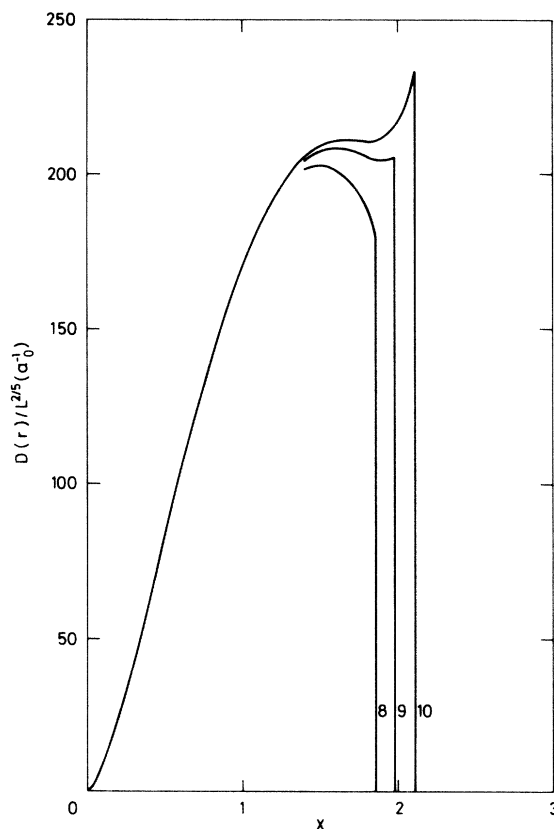


FIG. 7. Radial distributions of charge (divided by $L^{2/5}$), for $Z = 10$, $N = 8, 9, 10$, and $\Delta = -2$ (TFD calculation).

fects are important at the periphery of the atom, and they may modify considerably the binding energies of the outermost electrons, although they cannot affect much the total binding energy of a high- Z atom.

III. STATISTICAL MODEL WITH EXCHANGE

A. Exchange energy

In order to incorporate the exchange interaction in the model, we must give a statistical treatment both to the longitudinal and transverse motions. Thus, we shall assume that locally, inside a small cell of volume ΔV , the motion of an electron may be described by a superposition of plane waves of the form

$$u_{\vec{p}q}(\vec{p}, z) = (\Delta V)^{-1/2} \exp(i\vec{p} \cdot \vec{p} + iqz), \quad (37)$$

with $|\vec{p}| \leq p_F$, $|q| \leq q_F(\vec{r})$. In the spirit of the adiabatic approximation, the longitudinal and transverse Fermi momenta are taken to be independent; in fact, p_F should be determined by the magnetic field alone, and therefore be a constant, independent of the position of the cell. This is confirmed by a direct calculation: Counting the states inside ΔV we obtain a density of electrons

$$n(\vec{r}) = \frac{1}{(2\pi)^2} p_F^2 q_F(\vec{r}), \quad (38)$$

and comparison with Eq. (5) yields¹⁴

$$p_F^2 = 2eB. \quad (39)$$

Moreover, we remark that, within the range of validity of the model, we have

$$q_F(r_0) \ll p_F; \quad (40)$$

this is nothing else than Eq. (30), expressed in terms of the Fermi momenta.

Now, the exchange energy corresponding to our cell may be written as

$$\Delta W' = -\frac{e^2}{2} \frac{(\Delta V)^2}{(2\pi)^6} \int d\vec{p}_1 d\vec{p}_2 \int dq_1 dq_2 \Omega(\vec{p}_1 - \vec{p}_2, q_1 - q_2), \quad (41)$$

$$|\vec{p}_1|, |\vec{p}_2| \leq p_F; \quad |q_1|, |q_2| \leq q_F$$

where

$$\Omega(\vec{p}_1 - \vec{p}_2, q_1 - q_2) = \int d\vec{r}_1 d\vec{r}_2 u_1^*(1) u_2^*(2) \frac{1}{|\vec{r}_1 - \vec{r}_2|} u_1(2) u_2(1), \quad (42)$$

$$\vec{r}_1, \vec{r}_2 \in \Delta V;$$

for simplicity, we have used the shorthand notation

$$u_\alpha(\beta) = u_{\vec{p}_\alpha q_\alpha}(\vec{r}_\beta). \quad (43)$$

The integrations in Eq. (41) give

$$\Omega(\vec{p}, q) = \frac{4\pi}{\Delta V} \frac{1}{\vec{p}^2 + q^2}. \quad (44)$$

The elementary but tedious momentum integrations in Eq. (41) yield the final result

$$\Delta W' = -\frac{e^2}{2\pi^3} p_F^4 I(q_F/p_F) \Delta V, \quad (45)$$

where

$$I(\eta) = -\frac{1}{2}\eta^2 \ln \eta + \frac{1}{2}(1 - \ln 2)\eta^2 + O(\eta^3). \quad (46)$$

Collecting all the terms, we find the exchange energy density

$$w'(\vec{r}) = \frac{2\pi e^2}{eB} n^2(\vec{r}) [\ln \nu(\vec{r}) + C + O(\nu)], \quad (47)$$

where

$$\nu(\vec{r}) = \frac{n(\vec{r})}{(eB)^{3/2}}, \quad C = 2.32918; \quad (48)$$

the terms of order q_F/p_F and higher have been neglected, by virtue of Eq. (40).¹⁵

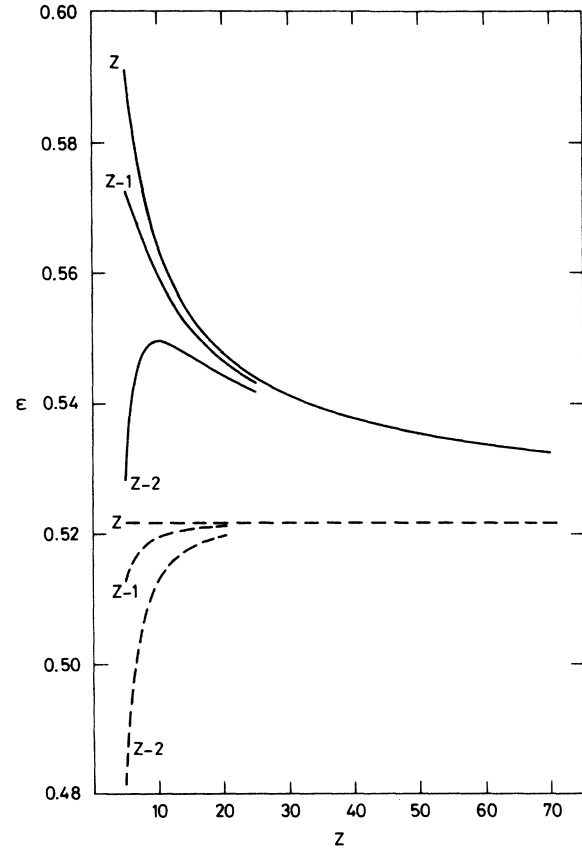


FIG. 8. Graphs of ϵ vs Z along the virial strip, for $N = Z - 2, Z - 1, Z$ (TFD calculation, solid curves); graphs of ϵ vs Z , for $N = Z - 2, Z - 1, Z$ (TF calculation, dashed curves).

B. Thomas-Fermi-Dirac equation

Including the exchange term, the energy of the atom becomes

$$E = K + V + W + W', \quad (49)$$

where the exchange energy is [neglecting contributions of order $O(\nu)$]

$$W' = \frac{2\pi e^2}{eB} \int n^2(\bar{r}) [\ln \nu(\bar{r}) + C] d\bar{r}. \quad (50)$$

Minimization with respect to $n(\bar{r})$ yields, instead of Eq. (11), the Thomas-Fermi-Dirac (TFD) integro-differential equation

$$\frac{2\pi^4}{m(eB)^2} n^2(\bar{r}) + e[\varphi(\bar{r}) - \varphi_0] + \frac{2\pi e^2}{eB} n(\bar{r}) [2 \ln \nu(\bar{r}) + 2C + 1] = 0. \quad (51)$$

Again, we assume spherical symmetry and, in order to obtain a differential equation, combine Eqs. (13) and (51). The definitions Eqs. (15) and (16) are maintained, but Eq. (22) no longer holds, because the exchange term in Eq. (51) has modified the relation between the potential and the electron density. Moreover, Eq. (51) cannot be solved explicitly for the electron density, and we have to introduce, in addition to $\Phi(x)$, a second function, $\Psi(x)$, defined by the relation

$$n(r) = a_0^{-3} 2^{-1/5} \pi^{-11/5} \alpha^{-12/5} Z^{2/5} L^{6/5} [\Psi(x)/x]^{1/2}, \quad (52)$$

$$\epsilon = -\frac{1}{2} \left\{ \Phi'(0) - \frac{1}{x_0} \left[\Phi(x_0) - \left(1 - \frac{N}{Z}\right) \right] \left(1 - \frac{N}{Z}\right) - \frac{1}{3} \int \Phi'' \Psi dx - 2^{1/5} \pi^{-4/5} \alpha^{2/5} Z^{-2/5} L^{-1/5} \int \Psi x dx \right\}. \quad (56)$$

The virial theorem reads

$$6K + V + W + W' = 0, \quad (57)$$

and in our model it is satisfied only approximately, because we have neglected higher-order terms in the expression of W' . Equation (27) is replaced by

$$3K + V + 2W + 2W' = e\varphi_0 N - \frac{2\pi e^2}{eB} \int n^2(\bar{r}) d\bar{r}, \quad (58)$$

where φ_0 is determined from Eq. (50), setting $r = r_0$:

$$\epsilon = -\frac{5}{9} \left\{ \Phi'(0) - \frac{1}{x_0} \left[\Phi(x_0) - \left(1 - \frac{N}{Z}\right) \right] \left(1 - \frac{N}{Z}\right) - 2^{1/5} \pi^{-4/5} \alpha^{2/5} Z^{-2/5} L^{-1/5} \int \Psi x dx \right\}. \quad (60)$$

which replaces Eq. (22). Written in terms of this parametrization, Eq. (13) becomes the TFD differential equation

$$\Phi'' = (x\Psi)^{1/2}, \quad (53)$$

the two functions being related by

$$\Phi = \Psi + 2^{1/5} \pi^{-4/5} \alpha^{2/5} Z^{-2/5} L^{-1/5} (x\Psi)^{1/2} \times [\ln(\Psi/x) - 1 + \ln(2^{13/5} \pi^{-2/5} \alpha^{6/5} Z^{4/5} L^{-3/5})], \quad (54)$$

which is a transcription of Eq. (51).

The boundary conditions (18) and (21) remain unchanged, but the atomic radius is no longer defined by Eq. (19). The position of the atomic boundary is found from the requirement that the pressure of the electron gas vanishes,¹⁶ which yields the following equation for x_0 :

$$\Phi(x_0) = -\frac{1}{3} \Psi(x_0) - 2^{1/5} \pi^{-4/5} \alpha^{2/5} Z^{-2/5} L^{-1/5} [x_0 \Psi(x_0)]^{1/2}. \quad (55)$$

The exchange term has mixed all the parameters, making the equations too complicated for a qualitative discussion. The solution of the TFD equation depends in an intricate manner upon Z , N , and L ; lengths and energies have no more a simple scaling behavior with respect to L . In particular, the energy, Eq. (49), may be written as in Eq. (23), where now

$$e\varphi_0 N = \frac{m\alpha^2}{2} 2^{8/5} \pi^{-2/5} \alpha^{-4/5} Z^{9/5} L^{2/5} \times \left\{ \frac{1}{x_0} \left[\Phi(x_0) - \left(1 - \frac{N}{Z}\right) \right] \frac{N}{Z} \right\}. \quad (59)$$

Using the virial theorem one can check the reliability of the approximation which consists in neglecting higher-order contributions in Eq. (50), in the following way. Assuming Eq. (57) to hold exactly, one has $E = -5K$; then, Eqs. (57) and (58) may be combined, eliminating $W + W'$, to yield a relation between K and V , and therefore an expression of E in terms of V and the quantities appearing in the right-hand side of Eq. (58). One obtains as a result of these manipulations

When exchange is neglected, both Eqs. (56) and (60) reduce to Eq. (24); however, they are not equal, and their difference tells us the degree of violation of the virial theorem, and therefore the accuracy of the expression (50) for the exchange energy.

C. Numerical results

Equations (53) and (54), with the boundary conditions (18) and (21), and x_0 defined by Eq. (55), were solved numerically inside the region shown, in a $\log Z$ - $\log L$ diagram, in Fig. 4. This region corresponds to the following ranges for the input variables.

- (i) Atomic number. $5 \leq Z \leq 20$ (steps of 1) and $20 \leq Z \leq 70$ (steps of 5).¹⁷
- (ii) Number of electrons: $Z - 2 \leq N \leq Z$.
- (iii) Magnetic field: $10^{-3} \leq L \leq 10^1$, with the restriction imposed by Eq. (31), in which the inequality signs were taken to mean "greater (smaller) or equal," and not "much greater (smaller)"; in other words, the calculation was pushed to the

extreme limits of validity of the model. In this range the magnetic field was given values equally spaced in logarithmic scale: $L = 10^\Delta$, $-3 \leq \Delta \leq 1$ (steps of 0.25).

Total atomic energies were calculated using both Eqs. (56) and (60), and the difference was found to be always less than 1%. Moreover, this difference vanishes along a curve contained inside the narrow strip in Fig. 4, showing that the virial theorem is obeyed exactly. This test confirms the accuracy of the approximation used for the exchange energy.

The exchange interaction reduces the electron repulsion, so that a given charge may be packed inside a smaller radius than predicted by the TF model. Indeed, for any given Z and N , and for all values of L inside the range of the model, x_0 is smaller than the corresponding TF value; moreover, as in the conventional TFD model, x_0 is finite even for neutral atoms. Its dependence on the magnetic field is practically negligible: Over the whole region shown in Fig. 4 it leads to

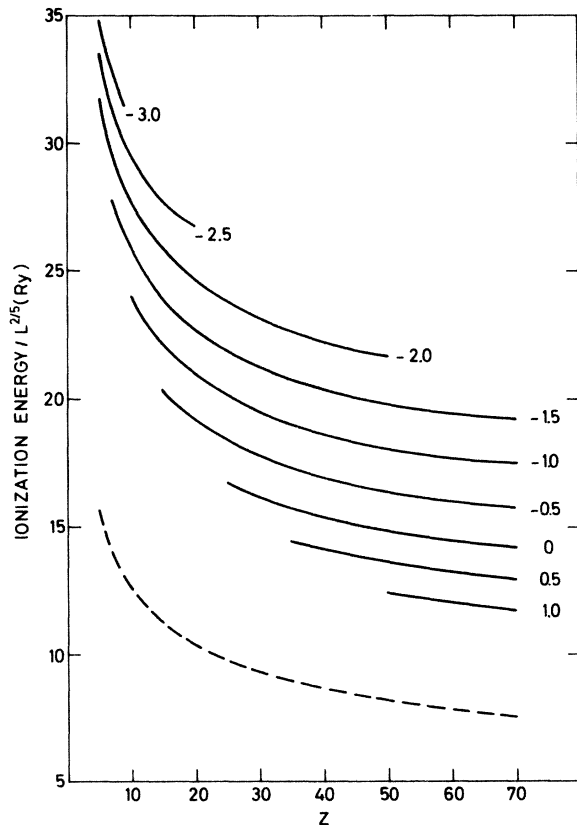


FIG. 9. Ionization energies of the Z th atomic electron (divided by $L^{2/5}$) vs Z : TFD calculation (solid curves; the numbers give the corresponding values of Δ) and TF calculation (dashed curve).

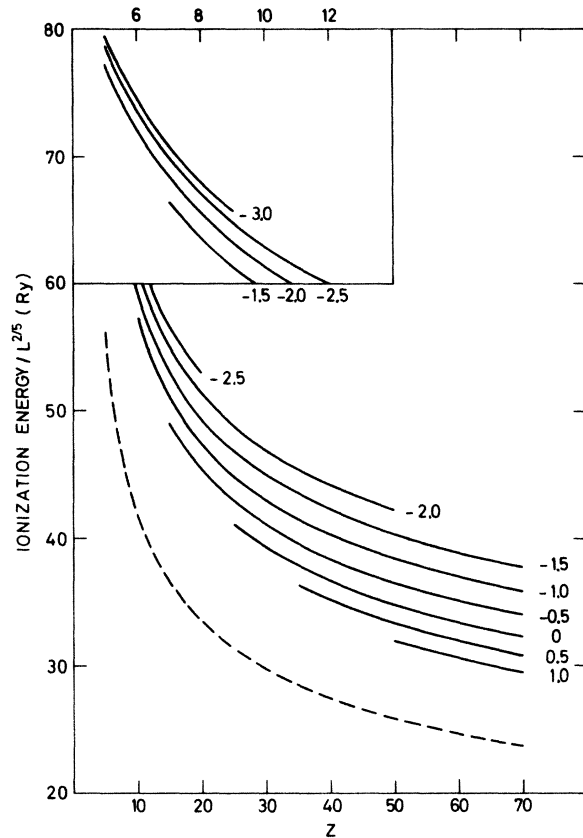


FIG. 10. Ionization energies of the $(Z-1)$ th atomic electron (divided by $L^{2/5}$) vs Z : TFD calculation (solid curves; the numbers give the corresponding values of Δ) and TF calculation (dashed curve).

variations less than 4%, so that the L dependence of the atomic radii is given essentially by the factor $L^{-2/5}$ in Eq. (15). Therefore, it is sufficient to report the values of x_0 along the "virial strip." In Fig. 5 these are plotted against Z , for $N=Z-2$, $Z-1$, Z ; for comparison, the corresponding TF curves for $N=Z-2$, $Z-1$ are also shown. With respect to the TF calculation, the radii are seen to be reduced by 10–15%, depending on the atomic number and the degree of ionization.

The solutions of the TFD equation for free ions are always of the type (i) discussed in Sec. II B. An example is given in Fig. 6, which shows the solution corresponding to $Z=10$, $N=9$, and $\Delta=-2$; to get a feeling of the modifications introduced by exchange, this should be compared with Fig. 1. Much more sensitive to these modifications is the physically relevant quantity $D(r)$, the radial distribution of charge. Figure 7 shows a plot of the function $D(r)/L^{2/5}$ against x , for $Z=10$, $N=8, 9, 10$, and $\Delta=-2$. A comparison with Fig. 2 reveals that near the nucleus the charge distribution is practically undisturbed by the exchange interaction, the contraction of the atom being achieved by squeezing the outer electrons. Two characteristic consequences of this fact are the discontinuous drop to zero of the density of charge at the boundary of the atom, and the sudden increase of $D(r)$ which precedes it, if the degree of ionization $1-N/Z$ is small enough.¹⁸

Like x_0 , the quantity ϵ —given by Eq. (56) or (60)—is practically independent of the magnetic field (variations with L amount to less than 1%, over the whole explored range), and energies increase essentially as $L^{2/5}$. The variation of ϵ with the atomic number, along the virial strip, is shown in Fig. 8, for $N=Z-2$, $Z-1$, Z , together with the corresponding TF curves. When exchange interactions are taken into account, ϵ becomes a decreasing function of Z , instead of an increasing one. The "anomalous" behavior of twice-ionized atoms with small Z has the same explanation as the absence of an increase of $D(r)$ near the atomic boundary, for $N=Z-2$, in Fig. 7: The degree of ionization being too high, Coulomb forces are very strong, and some of the typical effects of exchange do not show up. From Fig. 8 we learn that the contribution of the exchange to the binding energies of atoms decreases from 12% at $Z=5$ to less than 2% at $Z=70$.

The binding energies of the individual electrons at the periphery of the atom are extremely sensitive to the exchange terms, and for them the mixing of the magnetic and Coulomb effects introduced by exchange becomes significant. Figures 9 and 10 show the binding energies of the Z th and $(Z-1)$ th atomic electrons, divided by $L^{2/5}$, as

functions of the atomic number, for different values of the magnetic field; the corresponding TF curves are also given. The exchange contribution to the TFD ionization energies is of the order of 30–60%, depending on Z , N , and L ; its relative importance decreases with the increase of the magnetic field.

Qualitatively, exchange corrections decrease atomic radii and increase total binding energies, without affecting appreciably their dependence on the magnetic field, and smooth their dependence on the atomic number, at high Z . Ionization energies are increased by a quantity which depends on the magnetic field and tends to become independent of the atomic number, at high Z . The results presented in Figs. 5 and 8–10 may be extrapolated to higher atomic numbers, if the magnetic field is high enough for such an extrapolation to be meaningful.

IV. CONCLUSIONS

It is known that the conventional (zero magnetic field) statistical model of atoms cannot predict the oscillations of the ionization energies with the atomic number, which explain the periodicities in the chemical properties of elements. As for the question whether a similar situation might possibly occur also in a very strong magnetic field, the answer is, most probably, negative. In the superstrong range^{8–10} the shell structure leading to such oscillations is completely destroyed by the magnetic field; in the medium-strong range examined here the situation should be similar, even if the states at the disposal of the electrons are not the same. In the frame of the adiabatic approximation, which was used to define the term "very strong magnetic field" there is no room for a shell structure; only very small deviations from the smooth dependence of the ionization energies on the atomic number are conceivable, due to the details of the electronic configuration.

It has been pointed out¹⁰ that, by extrapolating the results of the Hartree calculation for the superstrong range and of the statistical model for the medium-strong range to the intermediate region, a good agreement is found for the atomic sizes and binding energies. Now, we find that such an agreement exists also for the ionization energies, within a factor of 2; this is a positive test for both the calculations.

Temperature effects have been neglected here; if temperatures are indeed of the order of 10^5 °K or less, such effects should be small, but they may still modify the ionization energies at low field intensities. Various other corrections and possible refinements of the model¹¹ are probably

of no great importance, and seem premature at this moment.

The emission of electrons and ions from the surface of a pulsar, and therefore the properties of its magnetosphere, depend in a crucial manner on the ionization energies calculated here. Also, if the speculation that pulsars are sources of cosmic rays¹⁹ proves to be correct, the knowledge of the ionization energies may help to provide a clue to the understanding of the distribution of the elements on the surface of a pulsar, from the knowledge of their abundances in the cosmic radiation. Other results of our work, e.g., the atomic sizes and binding energies, might be useful in the investigation of the properties of con-

densed matter on the surface of magnetic neutron stars.^{20,21}

ACKNOWLEDGMENTS

Two of the authors (B. B. and D. H. C.) wish to thank Professor L. A. Radicati for many stimulating discussions, and for his warm hospitality at the Scuola Normale Superiore, Pisa, where much of this work was done. The third-named author (P. R.) thanks Professor J. Ausländer for his kind hospitality at the Institut für Experimentelle Kernphysik der Universität and the Kernforschungszentrum, Karlsruhe.

*Present address: CERN, Geneva, Switzerland.

¹M. Ruderman, Phys. Rev. Lett. 27, 1306 (1971); Institute for Advanced Study, Princeton report, 1972 (unpublished).

²S. Tsuruta, V. Canuto, J. Lodenquai, and M. Ruderman, Astrophys. J. 176, 739 (1972).

³Due to translational invariance, the magnetic levels are infinitely degenerate.

⁴On units and notation, see the last paragraph of Sec. I.

⁵R. Loudon, Am. J. Phys. 27, 649 (1959); L. K. Haines and D. H. Roberts, *ibid.* 37, 1145 (1969).

⁶B. B. Kadomtsev, Zh. Eksp. Teor. Fiz. 58, 1765 (1970) [Sov. Phys.—JETP 31, 945 (1970)].

⁷R. O. Mueller, A. R. P. Rau, and L. Spruch, Phys. Rev. Lett. 26, 1136 (1971).

⁸R. Cohen, J. Lodenquai, and M. Ruderman, Phys. Rev. Lett. 25, 467 (1970).

⁹B. B. Kadomtsev and V. S. Kudryavtsev, Zh. Eksp. Teor. Fiz. Pis'ma Red. 13, 61 (1971) [JETP Lett. 13, 42 (1971)].

¹⁰D. H. Constantinescu and P. Reháč, Phys. Rev. D 8, 1693 (1973).

¹¹P. Gombás, *Die statistische Theorie des Atoms und ihre Anwendungen* (Springer, Vienna, 1949), is the standard reference. A good and concise review is found in H. A. Bethe and R. Jackiw, *Intermediate Quantum Mechanics*, 2nd edition (Benjamin, New York, 1968), Chap. 7.

¹²Because of this weak dependence upon N , very good accuracy is needed, if one wants to calculate ionization energies: In Eq. (25) we have the difference of two large numbers which are almost equal, and for high Z 's as many as four figures are lost.

¹³The similarities with the conventional TF model (see Sec. II B) are only qualitative: A very strong magnetic field keeps the electrons much closer to the nucleus than the Coulomb field, and the function $\Phi(x)$ decreases much faster than in the conventional case. Indeed, the x_0 's shown in Table I are about ten times smaller than

the conventional ones, and the solution for neutral atoms vanishes asymptotically faster than e^{-2x^2} , instead of behaving like $144x^{-3}$.

¹⁴Apart from the numerical factor, this is obvious from purely dimensional considerations.

¹⁵Of course, near the nucleus, where the electron density is singular, an expansion in terms of ν is meaningless. But near the nucleus the exchange interaction is irrelevant (compare Figs. 2 and 7) and, anyway, this region does not contribute to the charge and energy integrals. What matters is the region $r \approx r_0$, where the condition $q_F \ll p_F$ is satisfied.

¹⁶The pressure is given by $P = -(\partial u / \partial v)_S$, where u and v are, respectively, the energy and the volume per particle. Our model assumes zero temperature, hence the entropy is constant.

¹⁷For $Z > 70$, our iteration method turned out to converge badly, and the results are not accurate enough to be reported. However, in this region the quantities x_0 and ϵ , as well as the ionization energies, are already very weakly Z -dependent, so that our results may be easily extrapolated beyond $Z = 70$ (see Figs. 5 and 8–10).

¹⁸These effects reveal some of the shortcomings of the statistical model with exchange, and occur here as well as in the conventional TFD calculation (in this latter case the second effect is much less striking, being almost hidden in the tail of the charge distribution). For a discussion on this point, see N. H. March, Adv. Phys. 6, 1 (1957).

¹⁹A recent reference is C. F. Kennel, G. F. Schmidt, and T. Wilcox, Phys. Rev. Lett. 31, 1364 (1973). See also Ref. 8.

²⁰R. O. Mueller, A. R. P. Rau, and L. Spruch, Nat. Phys. Sci. 234, 31 (1971).

²¹D. H. Constantinescu and P. Reháč, paper presented at the Meeting on the Role of Magnetic Fields in Physics and Astrophysics, NORDITA, Copenhagen, June, 1974 (to be published).